

## Effect of Solvent on PL Spectra for Defect Analysis of CuO Nanoparticles

Md Jannatul Ferdous Anik<sup>1</sup>, Oishy Roy<sup>1</sup>, Hridoy Saha<sup>1</sup>, Md. Muktadir Billah\*

<sup>1</sup>Department of Materials and Metallurgical Engineering, Bangladesh University of Engineering and Technology, Dhaka 1000

\*Department of Materials and Metallurgical Engineering, Bangladesh University of Engineering and Technology, Dhaka 1000

---

### Abstract

Copper oxide (CuO) is one of the potential semiconductor metal oxides which has numerous possible applications in optoelectronic device applications. Nanoparticles (NPs) for such applications require high end optical characterization, for which photoluminescence (PL) spectroscopy is considered as one of the most important tools to reveal the optical and electronic band structures along with defects. The electron hole recombination rate and the defect structures are important criteria determining the performance of nanoparticles in such applications, i.e., photocatalytic degradation of dyes and to get insights into these parameters can help to explain the mechanism of photocatalytic degradation. One of the convenient ways to conduct PL spectroscopy of such nanoparticles is by dispersing in liquid solvent. However, due to solute-solvent interaction, characterization and analysis of PL spectra can be quite challenging sometimes as the PL intensity shows variation for the same NPs but dispersed in different solvents. In this study, CuO NPs were synthesized by co-precipitation method, characterized using x-ray diffraction (XRD), field emission scanning electron microscopy (FE SEM), ultra-violet visible spectroscopy (UV-Vis) and photoluminescence spectroscopy. Three different solvents were used for PL, which includes methanol, ethanol, and isopropanol. Finally, the effect of these solvents on PL spectra of the NPs was studied thoroughly.

*Keywords: Photoluminescence, Nanoparticles, Solvent, Photocatalysis, Defect.*

---

### 1. Introduction

Nanostructured materials have attracted considerable amounts of interest due to their unique properties and potential for use in various applications, such as optics, gas sensing, photocatalytic, antimicrobial activities, and so forth [1]. Transition metal oxide nanoparticles such as ZnO, CuO, and TiO<sub>2</sub> possess special physical and chemical properties due to the quantum size effect compared to their bulk counterparts [2].

In recent times, CuO nanoparticles, a p-type semiconductor material, have drawn a lot of interest among the potential materials as they exhibit promising optoelectronic performance, are environmentally benign, and perform well electrochemically. In addition, the inexpensive cost of the raw material is also helpful for scalability [3].

For CuO nanoparticle synthesis, numerous physical and chemical processes such as chemical precipitation, hydrothermal, sol-gel, thermal decomposition, and sonochemical synthesis have been

well-established. Among them, the chemical co-precipitation approach has shown to be an efficient and cost-effective method for manufacturing semiconductor nanoparticles.

Optical band and defect states play significant roles in determining the performance of the nanoparticles [4]. Though optical analysis such as photoluminescence spectroscopy has been performed elaborately to understand the underlying relations, the effect of solvent on PL spectra of CuO nanoparticles has not been studied extensively before. The study of the impact of different solvents on the photoluminescence (PL) spectra of CuO nanoparticles can yield significant knowledge on their optical properties and surface interactions [5]. In this study, methanol, ethanol, and isopropanol were used as solvents and their effect on PL spectra was studied.

### 2. Experimental Details

## 2.1 Materials

Chemical coprecipitation method was involved for the synthesis of CuO nanoparticles. Chemicals utilized for this purpose were copper acetate monohydrate  $[\text{Cu}(\text{CH}_3\text{COO})_2 \cdot \text{H}_2\text{O}]$  as precursor, sodium hydroxide  $[\text{NaOH}]$  as pH stabilizer, glacial acetic acid to restrict the hydrolysis of copper acetate, and deionized water (DI) for solution preparation.

## 2.2 CuO nanoparticle Synthesis

For the synthesis of CuO NPs,  $\text{Cu}(\text{CH}_3\text{COO})_2 \cdot \text{H}_2\text{O}$  was dissolved in deionized (DI) water, magnetically stirred continuously while maintaining solution temperature at 60C, after first 10 minutes 1mL glacial acetic acid was added and 60 minutes later sodium hydroxide was added dropwise to maintain pH at 7. Precipitates formed during this process were given 24 hrs to settle down completely. Precipitates were washed with DI water thoroughly for several times and finally with ethanol once using a centrifuge machine. After drying for 24 hr, nanoparticles were annealed at 400C for 1hr and then furnace cooled down to room temperature.

## 3. Characterization

XRD was performed using Rikagu X-ray diffractometer with  $\text{Cu-K}\alpha$  radiations ( $\lambda=0.15406$  nm) in 20–80-degree range for structural analysis. Morphological analysis was done with JEOL JSM-7600F field emission scanning electron microscopy (FE SEM). The optical band gap was calculated from absorbance data from PerkinElmer Lambda 365 ultraviolet visible spectrophotometer. PL spectra varying all three solvents (methanol, ethanol, and isopropanol) were recorded with Mini PL-110 ( $\lambda=224.3$ nm).

## 4. Results and Discussion

### 4.1 XRD Analysis

Fig 1 depicts the XRD pattern for CuO nanoparticles. Diffraction peaks at  $32.58^\circ$ ,  $35.59^\circ$ ,  $38.83^\circ$ ,  $48.87^\circ$ ,  $58.37^\circ$ ,  $61.64^\circ$ ,  $66.22^\circ$ ,  $68.12^\circ$ ,  $72.52^\circ$ ,  $75.22^\circ$  are associated with the (110), (002), (111), (202), (20-2), (11-3), (022), (31-1), (220) and (22-2) planes, respectively confirming the monoclinic crystal structure of CuO (JCPDS-48-1548) [6]. Impurity peaks related to  $\text{Cu}_2\text{O}$  and  $\text{Cu}(\text{OH})_2$  were not observed, indicating the successful synthesis of single phase CuO nanoparticles only. Later, average crystallite size was calculated using Debye-Scherrer equation:

$$D(\text{nm}) = \frac{.9\lambda}{\beta \cos\theta};$$

Here,  $\lambda$  is the wavelength of the radiation used in XRD (0.15406 nm),  $\beta$  is the full width at half maximum (FWHM). Average crystallite size was 22.59 nm with a crystallinity of 89.04 percent. Micro-strain was calculated utilizing Williamson-Hall (W-H) plot as showed in Fig 2. The straight line found from linear fitting was originated from the equation:

$$\beta \cos\theta = \frac{.9\lambda}{D} + 4\epsilon \sin\theta$$

The slope of the straight line ( $\epsilon$ ) represents the micro-strain in nanoparticles which is  $\sim 2.14 \times 10^{-3}$ . The y axis intercept length of W-H plot also been useful to calculate the crystallite size which is 25.39 nm: corroborating the previous calculation from Debye-Scherrer equation.

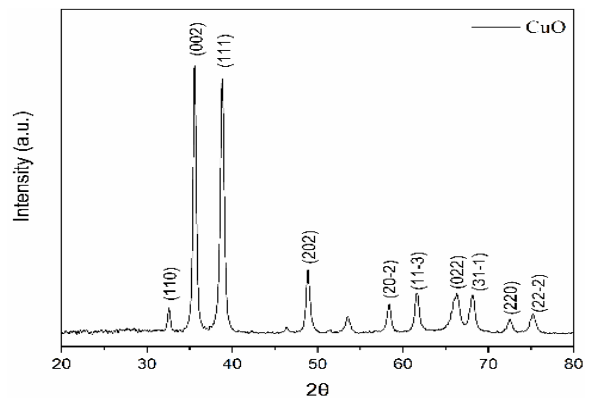


Fig 1: XRD peaks for CuO NPs

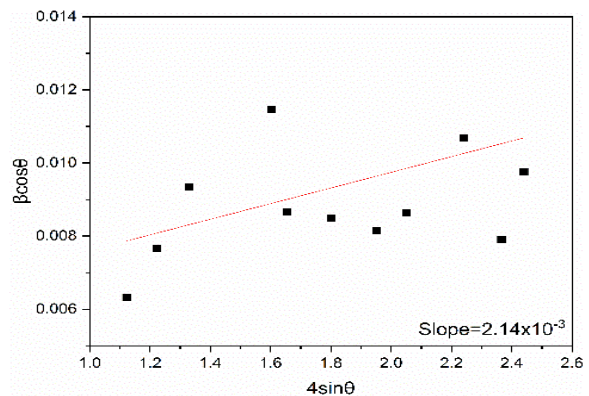


Fig 2: Williamson-Hall plot

### 4.2 Morphological Analysis

Morphological aspects of CuO nanoparticles synthesized from chemical co-precipitation method was revealed by FE SEM characterization. Fig 3 shows that nanoparticles have a nearly spherical shape with uniform distribution though some areas of the micrograph came with uneven aggregation as reported by few articles earlier [7]. Average particle size and distribution were measured using ImageJ and OriginLab pro software, respectively, illustrated in Fig 4. From FE SEM result, average particle size measured was 45.28 nm.

### 4.3 Optical Analysis

Optical properties were studied from the absorption and reflectance spectra of CuO nanoparticles over 400–1100 nm wavelength. The diffuse reflectance

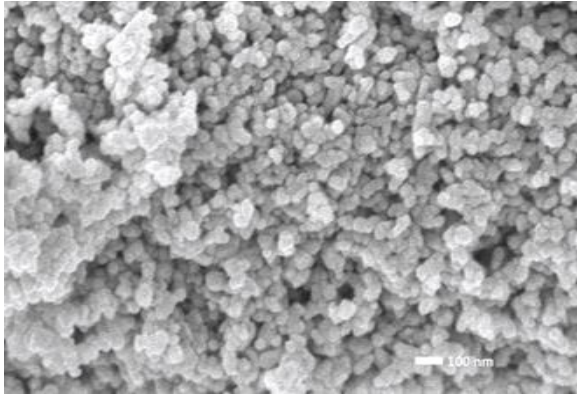


Fig 3: FE SEM image of CuO NPs

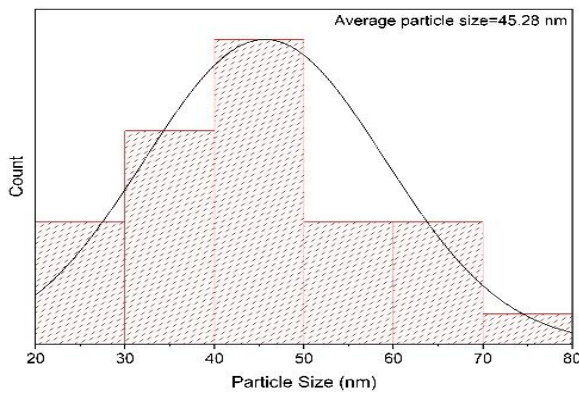


Fig 4: Particle size distribution

spectrum showed in Fig 5 exhibits a strong absorption at ~800 nm indicating the absorption edge of CuO in visible wavelength region. Optical band gap was measured from Tauc's plot following the formula:

$$ahv = (hv - E_g)^n$$

Here,  $E_g$  is the optical band gap,  $h\nu$  is the photon energy incident on particles,  $n$  is a constant which varies according to the optical transition; the values  $n$  is  $\frac{1}{2}$  and  $2$  for direct and indirect transition, respectively. In this study, an indirect band gap of 1.24 eV was found for the synthesized CuO nanoparticles as shown in Fig 6 [8].

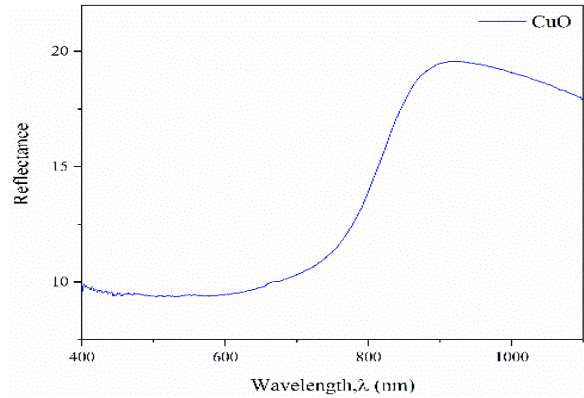


Fig 5: Reflectance Spectrum.

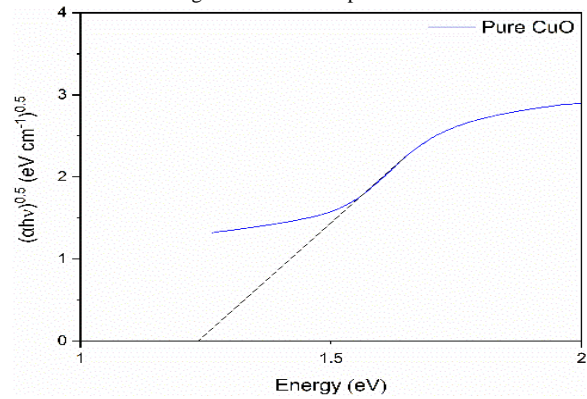


Fig 6: Indirect band gap of CuO

### 4.4 Photoluminescence study

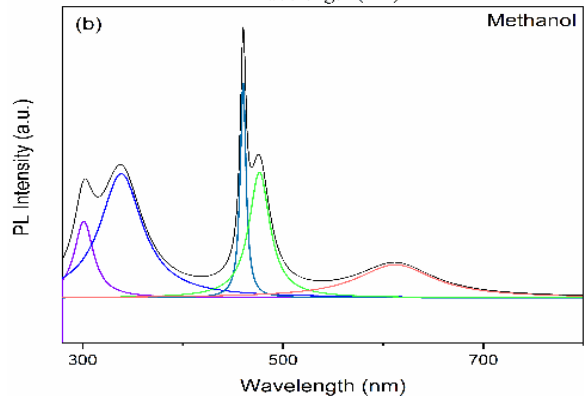
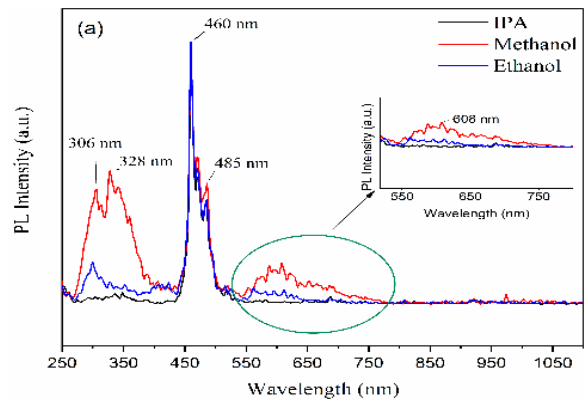


Fig 7: (a) PL spectra for CuO NPs in different solvents, (b) deconvoluted PL spectra for CuO demonstrating emission regions using methanol solvent.

Photoluminescence (PL) spectra of CuO nanoparticles were recorded in three different solvents, including methanol, ethanol, and isopropanol, and were excited at an optimal wavelength of 224 nm in the range of 250 nm to 1100 nm to investigate the band structure of the CuO nanoparticles and the presence of defect-related levels within the band structure showed in Fig 7. PL spectra for the CuO nanoparticle showed three prominent peaks at 328 nm, 460 nm, and 608 nm along with shoulder peaks appeared at 306 nm and 485 nm indicating CuO emission [9]. Peaks at UV region correspond to the near band edge emission (NBE) of free excitons in the conduction band while the prominent peak at violet to blue region is responsible for the singly ionized Cu vacancies [10-11]. A broad peak observed at around 608 nm attributed to the recombination of electrons and holes at singly ionized oxygen vacancies indicates deep level emission of CuO nanoparticles [12-13]. PL intensity of the nanoparticles increased with increasing dielectric constant of the solvents and PL intensity of CuO nanoparticles dissolved in methanol showed maximum intensity which indicates strong relation between the polarity of the solvent and the PL spectra. The radiative electron-hole recombination might be facilitated by more polar solvent methanol (dielectric constant = 32.7) compared to ethanol (dielectric constant = 24.5) and isopropanol (dielectric constant = 17.9), resulting in enhanced quantum yield. Earlier studies on CuO and SnO<sub>2</sub> [14] nanoparticles reported this phenomenon due to solute-solvent interaction or due to the variation in polarity of the solvents.

## 5. Conclusions

In brief, the synthesis of CuO nanoparticles was effectively achieved using the chemical co-precipitation route. The monoclinic crystalline phase of CuO was validated using X-ray diffraction (XRD), revealing a crystallite size of 22.59 nm. The band gap of the nanoparticles was determined using Tauc's formula, yielding a value of 1.24 eV. The analysis conducted using FE SEM demonstrated that the nanoparticles exhibited a mostly uniform spherical morphology. However, it should be noted that some degree of agglomeration was seen in the FE SEM micrograph. The intensity of emissions exhibited variability across various solvents as shown in the photoluminescence (PL) spectra. This suggests that the polarity of the solute-solvent interaction, and therefore the intensity of the PL spectra, is influenced by the solvent's polarity.

## References

[1] T. Naseem and T. Durrani, "The role of some important metal oxide nanoparticles for

wastewater and antibacterial applications: A review," *Environmental Chemistry and Ecotoxicology*, vol. 3, pp. 59–75, 2021, doi: 10.1016/j.eneco.2020.12.001.

- [2] K. Borgohain, J. B. Singh, M. V. Rama Rao, T. Shripathi, and S. Mahamuni, "Quantum size effects in CuO nanoparticles," *Phys. Rev. B*, vol. 61, no. 16, pp. 11093–11096, Apr. 2000, doi: 10.1103/PhysRevB.61.11093. Winterbourn, C. C. (2008). Reconciling the chemistry and biology of reactive oxygen species. *Nature Chemical Biology*, 4(5), 278–286. <https://doi.org/10.1038/nchembio.85>
- [3] Sagadevan, S., Pal, K. & Chowdhury, Z.Z. Fabrication of CuO nanoparticles for structural, optical and dielectric analysis using chemical precipitation method. *J Mater Sci: Mater Electron* 28, 12591–12597 (2017). <https://doi.org/10.1007/s10854-017-7083-3> <https://doi.org/10.1002/adem.201700270>
- [4] H. Mallick, Y. Zhang, J. Pradhan, M. P. K. Sahoo, and A. K. Pattanaik, "Influence of Particle Size and Defects on the Optical, Magnetic, and Electronic Properties of Al Doped SiO<sub>2</sub> Particles," *Journal of Alloys and Compounds*, vol. 2020, pp. 2–4, 2020, doi: 10.1016/j.jallcom.2020.156067.
- [5] Horti, N. C., Kamatagi, M. D., Patil, N. R., Wari, M. N. & Inamdar, S. R. Photoluminescence properties of SnO<sub>2</sub> nanoparticles: Effect of solvents. *Optik* 169, 314–320 (2018).
- [6] D. Singh et al., "Bacteria assisted green synthesis of copper oxide nanoparticles and their potential applications as antimicrobial agents and plant growth stimulants," *Front. Chem.*, vol. 11, p. 1154128, Apr. 2023, doi: 10.3389/fchem.2023.1154128.
- [7] Abd. Rahim Abu Talib, Sadeq Salman, Muhammad Fitri Mohd Zulkeple, and Ali Kareem Hilo, "Experimental Investigation of Nanofluid Turbulent Flow Over Microscale Backward-Facing Step," *ARFMTS*, vol. 99, no. 2, pp. 119–134, Nov. 2022, doi: 10.37934/arfmts.99.2.119134.
- [8] Y. Wang et al., "Electronic structures of Cu<sub>2</sub>O, Cu<sub>4</sub>O<sub>3</sub>, and CuO: A joint experimental and theoretical study," *Phys. Rev. B*, vol. 94, no. 24, p. 245418, Dec. 2016, doi: 10.1103/PhysRevB.94.245418.
- [9] P. Chand, A. Gaur, and A. Kumar, "Structural, optical and ferroelectric behavior of CuO nanostructures synthesized at different pH values," *Superlattices and Microstructures*, vol. 60, pp. 129–138, Aug. 2013, doi: 10.1016/j.spmi.2013.04.026
- [10] A. Muthuvel, M. Jothibas, and C. Manoharan, "Synthesis of copper oxide

- nanoparticles by chemical and biogenic methods: photocatalytic degradation and in vitro antioxidant activity,” *Nanotechnol. Environ. Eng.*, vol. 5, no. 2, p. 14, Aug. 2020, doi: 10.1007/s41204-020-00078-w.
- [11] R. Gopalakrishnan and M. Ashokkumar, “Rare earth metals (Ce and Nd) induced modifications on structural, morphological, and photoluminescence properties of CuO nanoparticles and antibacterial application,” *Journal of Molecular Structure*, vol. 1244, p. 131207, Nov. 2021, doi: 10.1016/j.molstruc.2021.131207.
- [12] A. Aslani, “Controlling the morphology and size of CuO nanostructures with synthesis by solvo/hydrothermal method without any additives,” *Physica B: Condensed Matter*, vol. 406, no. 2, pp. 150–154, Jan. 2011, doi: 10.1016/j.physb.2010.10.017.
- [13] M. Ponnar, C. Thangamani, P. Monisha, S. S. Gomathi, and K. Pushpanathan, “Influence of Ce doping on CuO nanoparticles synthesized by microwave irradiation method,” *Applied Surface Science*, vol. 449, pp. 132–143, Aug. 2018, doi: 10.1016/j.apsusc.2018.01.126.
- [14] K. Thirumurugan, K. Ravichandran, R. Mohan, S. Snega, S. Jothiramalingam, and R. Chandramohan, “Effect of solvent volume on properties of SnO<sub>2</sub>:Al films,” *Surface Engineering*, vol. 29, no. 5, pp. 373–378, Jun. 2013, doi: 10.1179/1743294412Y.0000000110.